Journal of *Marine Science and Engineering*

MDPI

Article

Desulfurizing of Pyrolysis Oil of Used Tires Using a 3D-Printed Vortex Diode and Modeling of Process

Jochen Uebe *, Žilvinas Kryževičius, Jolanta Janutėnienė, Audronė Žukauskaitė, Eugenijus Bertašius, Rokas Rapolavičius, Valdas Jankūnas and Audrius Senulis

Engineering Department, Faculty of Marine Technology and Natural Sciences, Klaipeda University, H. Manto 84, 92294 Klaipeda, Lithuania; zilvinas.kryzevicius@ku.lt (Ž.K.); jolanta.januteniene@ku.lt (J.J.); audrone.zukauskaite@ku.lt (A.Ž.); eugenijus.bertasius@gmail.com (E.B.); r.rapolavicius@gmail.com (R.R.); valdas.jankunas@ku.lt (V.J.); audrius.senulis@ku.lt (A.S.)

* Correspondence: jochen.uebe@ku.lt

Abstract: The use of pyrolysis oil can be seen as an alternative fuel for maritime transport. However, pyrolysis oil from tires must be desulfurized for this. Recently, this can be done by hydrodynamic cavitation. This process does not require oxidation chemicals but only water, a cavitation generator, and a pump to drive it. In the literature, this concept has been successfully tested on model fuels. In this study, the cavitation generator for the desulfurization of waste tire pyrolysis oil was printed from polylactic acid-based on simulations of the optimal design, which allows for much cheaper production and easy replacement in case of wear or testing of alternative designs. After 60 min of treatment at 5 bar inlet pressure, a desulfurization of almost 33% was achieved. Furthermore, an interaction analysis showed that only from a pyrolysis oil content of 5.5 to 6% does hydrodynamic cavitation have an effective effect on desulfurization.

Keywords: pyrolysis oil; used tires; fluid dynamics simulations; hydrodynamic cavitation

Citation: Uebe, J.; Kryževičius, Ž.; Janutėnienė, J.; Žukauskaitė, A.; Bertašius, E.; Rapolavičius, R.; Jankūnas, V.; Senulis, A. Desulfurizing of Pyrolysis Oil of Used Tires Using a 3D-Printed Vortex Diode and Modeling of Process. *J. Mar. Sci. Eng.* **2021**, *9*, 876. https://doi.org/10.3390/jmse9080876

Academic Editor: Tie Li

Received: 9 July 2021
Accepted: 7 August 2021
Published: 13 August 2021

1. Introduction

A significant proportion of world trade is conducted via maritime transport [1], and according to [2], it is arguably the most cost-effective way to transport goods around the world. In 2018, the International Maritime Organization (IMO) announced ambitious plans to reduce greenhouse gases emissions from international shipping by half by 2050 compared to 2008 levels [3]. The decarbonization of shipping can be achieved in a number of ways: through the use of alternative fuels, solar and wind energy, through technological tools that help increase energy usage efficiency, through improving activity, e.g., more accurately regulating vessel speeds, creating more accurate routings, etc. Alternative fuels have the potential to reduce carbon dioxide (CO_2) emissions and, in some cases, depending on what they were from, can even have zero emissions [4,5]. Nevertheless, any alternative fuel must comply with a series of criteria to become perspective in the future. The most important criterion is reducing emissions in the whole life cycle of the fuel. After evaluating alternative fuel potentials to reduce greenhouse emissions, it was determined that reaching wanted levels of decarbonization is very difficult with the currently available alternatives. Certain alternatives, such as liquified natural gas (LNG), reduce the greenhouse emissions in no significant way, while hydrogen does not emit greenhouse gas during use, but after assessing the whole life cycle, greenhouse emissions during the production phase are to be taken into account. Therefore, there is no unilateral solution, and the search for new alternatives is very important [6].

Pyrolysis oil, e.g., from tires, could be an environmentally friendly and economical fuel for the propulsion of maritime transport [7]. In the European Union (EU), landfilling of used tires has been banned for several years [8] and is, therefore, problematic [9]. Nevertheless, used tires in the EU still end up in landfills or are otherwise disposed of illegally. Globally,

this problem is far greater [10,11]. Tires made of rubber cannot be melted to be reused due to the thermally irreversible cross-linking by sulfur [11,12].

Current literature mostly focuses on high temperatures and heating rates in laboratories and powdery feedstock, thus simplifying the highly complex pyrolysis process [13]. However, pyrolysis processes are rather uneconomical, dangerous and they can also produce highly toxic gases that require treatment before being discharged into the atmosphere. In pyrolysis processes for larger quantities, furnaces with very different designs are usually used so that part of the feedstock is thermally degraded under different conditions [14]. To increase the production of high-quality liquid products (fuel), the concept of slow pyrolysis can be applied. Slow pyrolysis is traditionally used to produce charcoal, whereby the vapors are either released into the atmosphere or burnt. The product yield depends in particular on the composition of the starting material [15], the dimensions of the starting particles [16], the heating rate, the final temperature [17], and the total reaction time. A few plants recover a limited number of chemicals from liquid by slow pyrolysis, such as acetic acid from the Chemviron plant in Germany [18,19]. However, recent developments in the field of slow pyrolysis show that especially the long duration of heat transfer, better control of inlet, and outlet flow rates (controlled product collection) can be an advantage of slow pyrolysis over fast pyrolysis to increase the production of high-quality liquid products [20].

Pyrolysis of waste tires would be a more environmentally friendly option [21–23] and has good characteristics for its valorization [24]. Used tires are an attractive source of alternative energy due to their long hydrocarbon chains with high calorific value [25], and material recycling is preferable to thermal recycling [26,27]. The use of tire pyrolysis oil in diesel engines as an alternative fuel has already been tested [28,29]. However, the condensed pyrolysis oil from used tires contains a relatively high amount of sulfur compounds (usually a few percent by weight) [11,30,31], which is not suitable for use in internal combustion engines according to European Union restrictions [25]. The general sulfur limit for fuels in European seas has dropped from 3.5% previously to 0.5% since the beginning of 2020. Fuel used in the Baltic Sea, the North Sea, and the English Channel—the so-called Sulphur Emission Control Areas (SECAs) of Europe- meet a sulfur limit of 0.1% (before 2015, it was allowed to be 1%). The limits can be met by using cleaner fuels or technologies such as scrubbers [3,32].

Various methods are used for desulfurization:

- Catalytic hydrodesulfurization is most commonly used in industry for the desulfurization of fuels. Catalysts based on Co-Mo or Ni-Mo are used at high temperatures and high pressures. In this way, sulfur contents of about 350 ppm are achieved, with special catalyst improvements even less [33];
- Oxidative methods, on the other hand, allow mild reaction conditions using oxygen or peroxides as well as catalysts [34], which, however, require a high loading with the oxidant;
- Extractive methods [35] use special solvents for sulfur-containing compounds in which non-sulfur hydrocarbons are less soluble as well as unconventional methods;
- Furthermore, there are special methods such as biological desulfurization, electrochemical treatments, desulfurization with metallic sodium, treatment with caustic solutions, etc. [36].

A detailed overview of the different desulfurization methods for oil is shown in [37].

A novel approach to the deep desulfurization of fuels is desulfurization by means of hydrodynamic cavitation [38]. According to [39,40], hydrodynamic cavitation is capable of providing economical, efficient, and environmentally friendly chemical, ecological and biological applications. A theoretical background is given, for example, in [41–43]. In this work, a modified system according to [38] is used, which employs a vortex diode to accelerate the flow velocity of the fluid based on water and fuel. At the output of the vortex, the diode is a Venturi tube which, in conjunction with the high flow velocity, creates cavitation bubbles in the center of the vortex. When the bubbles implode, high temperature and high pressure are generated, which lead to the formation of hydroxyl radicals [38,44,45].

Under these locally extreme conditions, the hydroxyl radicals remove the sulfur from the organic phase without any catalyst, and additional oxidation compounds; [38] used a model fuel of n-octane or commercial diesel, thiophene, and n-octanol and was able to achieve almost complete desulfurization. The cavitation system only requires water as an additional chemical to the fuel (the use of additional oxidants as in [46] is currently excluded for technical implementation by the US patent [47]), with energy input only via the pump.

For this study, used tires were pyrolyzed into a sulfurous oil. The pyrolysis oil, which is immiscible with water, was treated for desulfurization using hydrodynamic cavitation. For this purpose, a plant was constructed according to [38]. To determine the optimal geometric parameters of the Venturi tube of the cavitation tool, a fluid dynamic simulation was carried out with the SOLIDWORKS software. With the geometric parameters for maximum steam yield determined in this way, a Venturi tube was printed, and the desulfurization effect of the cavitation system on the pyrolysis oil was investigated under different process conditions.

2. Materials and Methods

2.1. Numerical Simulation of Fluid Dynamics

In a preliminary study, the entire cavitation tool was designed accordingly [48] and 3D printed after. It turned out that the Venturi tube does not work as efficiently as [38] describes. Therefore, using numerical simulations, we performed a geometric optimization based on the simplest form of Bernoulli's equation as given in [41,42] to achieve a higher cavitation rate.

The numerical modeling of turbulent flow with hydrodynamic cavitation presence was realized using software SOLIDWORKS (Dassault Systèmes SolidWorks Corporatio, Waltham, MA, USA), which employs the finite volume method to domain discretization.

The cavitation conditions depend on the ratio of the diameter of the axial tube D to the height of the chamber d, where the height of the chamber is also equal to the diameter of the entrance to the chamber. In the work of [49], it was deduced that the optimal value D/d is in the range 4.0~4.5. Following these recommendations, a model of vortex diode was created (Figure 1), and a numerical simulation of hydrodynamic cavitation was performed. In this work, geometrical parameters were changed: the pipe length L, throat tube diameter d, tube diameter D, rounding radius R of the throat influence were investigated as also being the influence of inlet pressure p and flow rate Q.

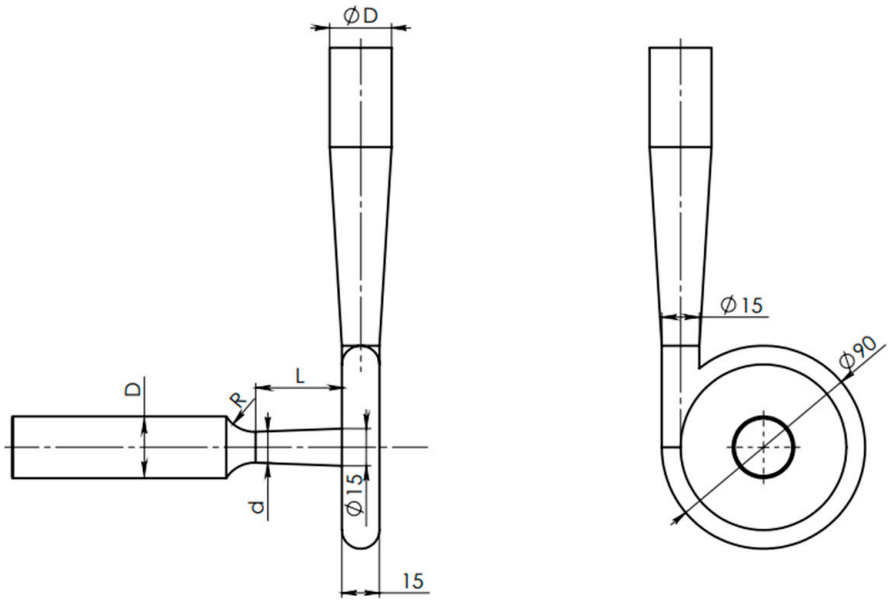

Figure 1. Schematic of vortex diode.

Initial data required for modeling are pressure p_o—entering the cavitator, initial flow rate Q at entering the cavitator, and leaving the cavitator.

The simulation results show the part of the mass vapor m_v due to cavitation as well as the expansion of the vapor volume in the tube when the tube diameter downstream of the throat of the Venturi tube is equal to D again.

2.2. Materials

Pyrolysis oil from waste tires (pyrolysis data are not included in this paper) with a total sulfur content of 10538 ppm was used for the desulfurization study. The water was deionized with GenPure Water Purification Systems (Thermo Fisher Scientific, Waltham, MA, USA).

2.3. Hydrodynamic Cavitation Setup

Vortex Venturi type tube hydrodynamic cavitation reactor system was printed using polylactic acid (PLA) based on the simulation results, which allow for much cheaper production and easy replacement in case of wear or testing of alternative designs. The Venturi tube is exchangeably integrated into the housing behind the vortex diode. The hydrodynamic cavitation system was made of a centrifugal pump (Italy E-Tech, Model EH5/09 I022 T5 E0 IE3; stainless steel, Qmax 117 L min^{-1}, 2.29 kW, 3 phase, 50 Hz motor, 2.29 kW), a holding tank equipped with a cooling system to maintain the temperature, and measuring devices (temperature, pressure). The system was designed to be capable of regulating pressure through a bypass line and manual valves on each branch. All piping was constructed to withstand 10 bar pressure, with pressure measured continuously with a pressure measurement device placed at the entrance of the cavitation tube. The hydrodynamic cavitation reactor system is depicted in Figure 2.

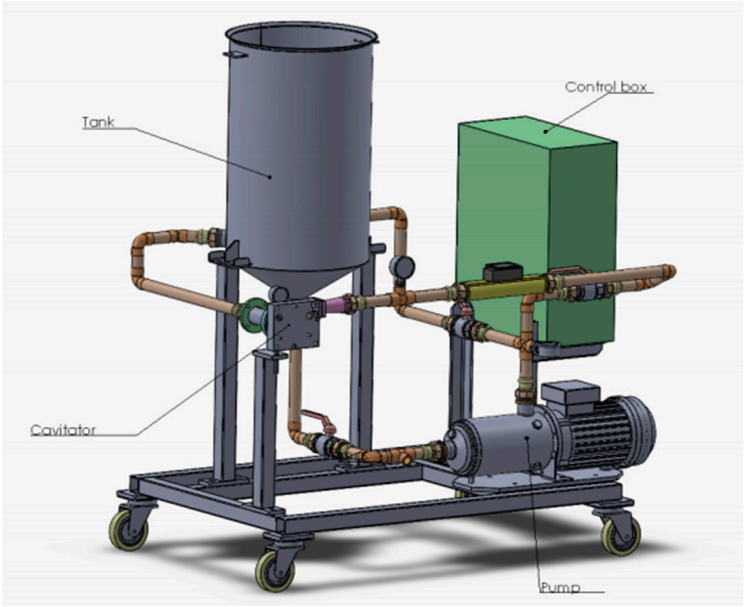

Figure 2. Details of experimental setup involving hydrodynamic cavitation system.

The liquid mixture is led from the tank container to the pump, which returns it at a certain pressure via the hydrodynamic cavitation reactor system. Additional mixing takes place in the tank to prevent the separation of the two phases.

2.4. Performing Desulfurisation

The three independent variables, process pressure, pyrolysis oil content in oil-water mixture, and process time, were studied for the effect of desulfurization. The ranges of the variables were established as such: process pressure of 3, 4, and 5 bar; pyrolysis oil

content in an oil-water mixture of 2.5, 5.0, and 7.5% and process times of 10, 20, 30, 40, 50, and 60 min, respectively.

For each experiment, 15 L of oil and water mixture were used. During the reaction stage, the temperature was kept at 40 ± 5 °C through the cooling system because, according to [50], cavitation decreases with increasing temperatures. Samples were taken periodically without stopping the process in the reactor. The samples were separated from the water by centrifugation at 3000 rpm for 15 min to separate water and oil phases. The total sulfur content of the waste tires pyrolysis oil and treated samples were determined using Energy Dispersive X-ray Fluorescence (EDXRF) elemental analyzer (Rigaku NEXQC, Japan) according to the ASTM D4294. Sulfur removal was calculated based on the initial and final obtained sulfur content according to Equation (1):

$$\text{Extent of Desulfurization (\%)} = (S_{initial} - S_{final})/S_{initial} \times 100 \quad (1)$$

3. Results and Discussions

3.1. Numerical Modeling and Analysis of the Cavitation Phenomenon in Vortex Tube

Numerical simulations were performed using the software SOLIDWORKS to select the conditions under which the cavitation process occurs. The parameters were changed during the simulation:

(a) geometric parameters of the tube length L from 25 to 40 mm, the throat diameter d from 7 to 12 mm, the tube diameter D from 22 to 28 mm, and the rounding radius R from 8 to 20 mm.

(b) working modes: pressure p from 3 to 12 bar and flow rate Q from 1.5 to 4 $m^3\ h^{-1}$.

About 360 simulations were performed. The simulation results of the several cases are presented in Table 1.

As we can see from the data presented in the table, the process is sensitive to changes in pressure and flow. Few examples of the simulation results are presented in Figures 3–6 based on the data in Table 1. The simulation results showed that cavitation does not excite at pressure 5 bar and a flow rate of 2.5 $m^3\ h^{-1}$, when L—40 mm, d—11 mm, D—26 mm, R—16 mm. Figures 3 and 4 show the results when a cavitation phenomenon occurs at the same pressure of 5 bar and when changing the flow rate (3.0–3.5 $m^3\ h^{-1}$); this indicates the mass fraction of vapor m_v.

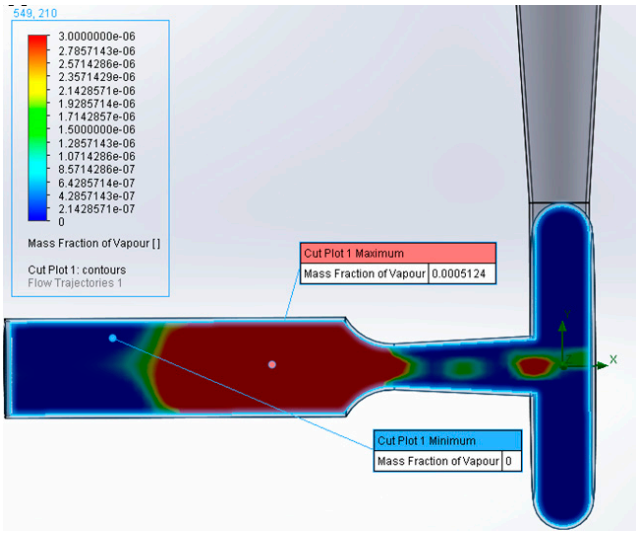

Figure 3. Cavitation in vortex diode, when p—5 bar, Q—3.0 m^3/h.

Table 1. Results of numerical simulation.

Geometrical Parameters of Vortex Diode				Working Modes		Cavitation	
Length of the Tube between Vortex Diode and the Throat L, mm	Diameter of Venturi Tube at the Throat d, mm	Rounding Radius of the Throat R, mm	Diameter of Inlet/Outlet Tube D, mm	Inlet Pressure p, Bar	Inlet Flowrate Q, $m^3\ h^{-1}$	Mass Fraction of Vapor, m_v	Length of Cavitation Bubbles Cloud after Throat Lcav, mm
40	11	16	26	5	2.5	0	0
40	11	16	26	5	3	0.0005124	120
40	11	16	26	5	3.2	0.0005166	135
34	10	12	26	6	2	0	0
34	10	12	26	6	2.5	0	0
34	10	12	26	6	3	0.0006797	90
34	10	12	26	6	3.2	0.0007837	100
34	10	12	26	4	2	0	0
34	10	12	26	4	2.5	0.0006159	110
34	10	12	26	4	3	0.0006117	150
34	10	14	26	6	2.5		
34	10	14	26	6	3	0.0005085	90
34	10	14	26	6	3.2	0.0007664	130
34	10	10	26	4	2	0	0
34	10	10	26	4	2.5	0.0006278	100
34	10	10	26	4	3	0.0006433	150
34	10	10	22	6	2.5	0	0
34	10	10	22	6	2.7	0.000004	51
34	10	10	22	6	3	0.0005485	90
35	12	12	26	6	2.5	0	0
35	12	12	26	6	3	0.0002774	90
35	12	12	26	6	3.5	0.0006468	150
40	11	14	26	4	2.3	0	0
40	11	14	26	4	2.5	0.0002098	130
25	7	8	20	3	2.4	0.0011306	150

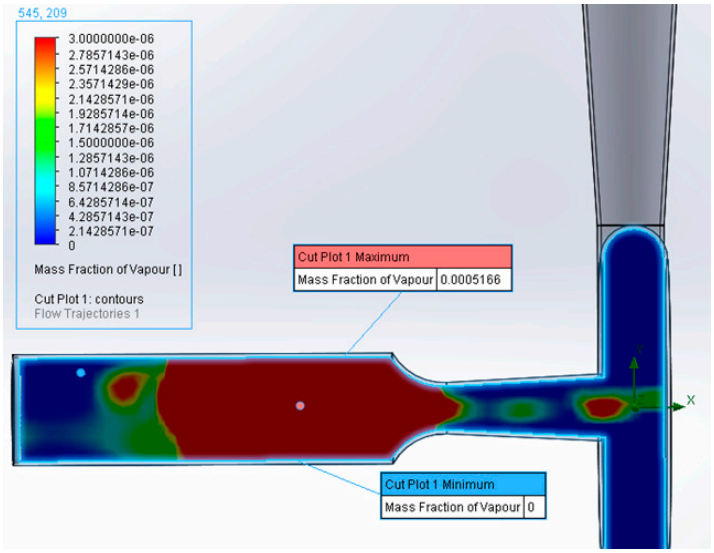

Figure 4. Cavitation in vortex diode, when p—5 bar, Q—3.2 m^3/h.

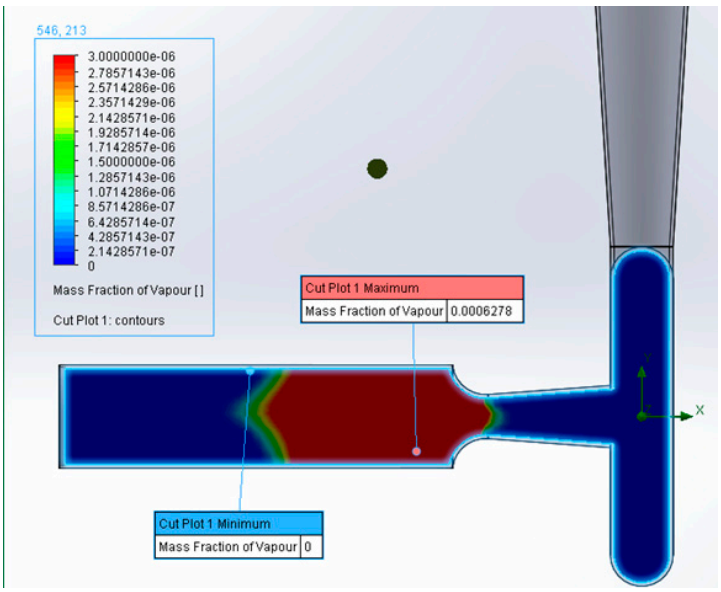

Figure 5. Cavitation in vortex diode, when p—4 bar, Q—2.5 m^3/h.

Similar results we can see after changing geometrical parameters l—34 mm, d—10 mm, D—26 mm, R—10 mm. When pressure p is 4 bar, and flow rate Q is 2.0 $m^3\ h^{-1}$, cavitation does not excite. However, if the flow rate is increased to 2.5–3.0 $m^3\ h^{-1}$ at the same pressure of 4 bar, cavitation occurs again (Figures 5 and 6).

As we can see from the simulation results, the change in flow rate Q has a greater effect on the excitation of the cavitation; therefore, there is no need to develop high pressure on the cavitation tool to extract cavitation conditions. The dependence of the mass fraction of vapor in m_v on pressure p and flow rate Q is presented in Figure 7.

The results of numerical simulation showed that the cavitation phenomenon is excited in the pressure range 3–6 bar and flow rate range 2.5–4 $m^3\ h^{-1}$.

Investigation of the vortex diode has shown that the optimal geometric parameters at which the highest mass fraction of steam in m_v is at the lowest energy consumption of 3 bar pressure and a flow velocity of 2.2 $m^3\ h^{-1}$. The geometrical parameters of the Venturi tube are then L—25 mm, d—7 mm, D—20 mm, and R—8 mm.

Based on these parameters, a Venturi tube with these geometric parameters was 3D printed for further experimental investigations.

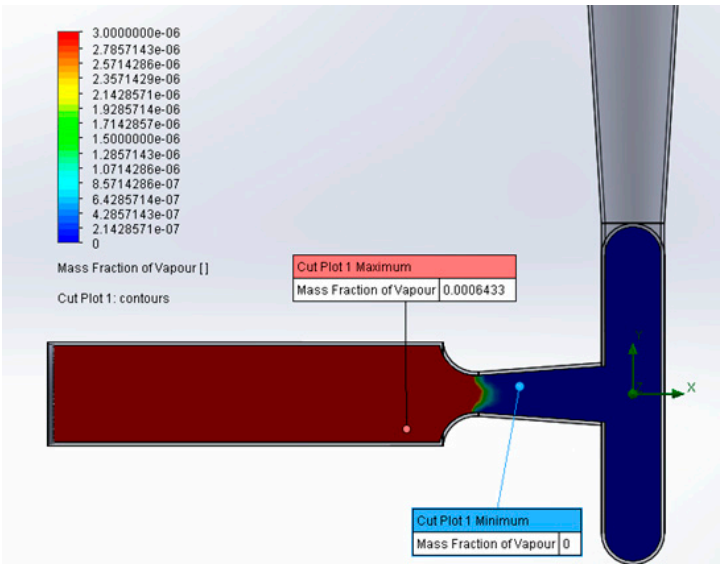

Figure 6. Cavitation in vortex diode, when p—4 bar, Q—3.0 m^3/h.

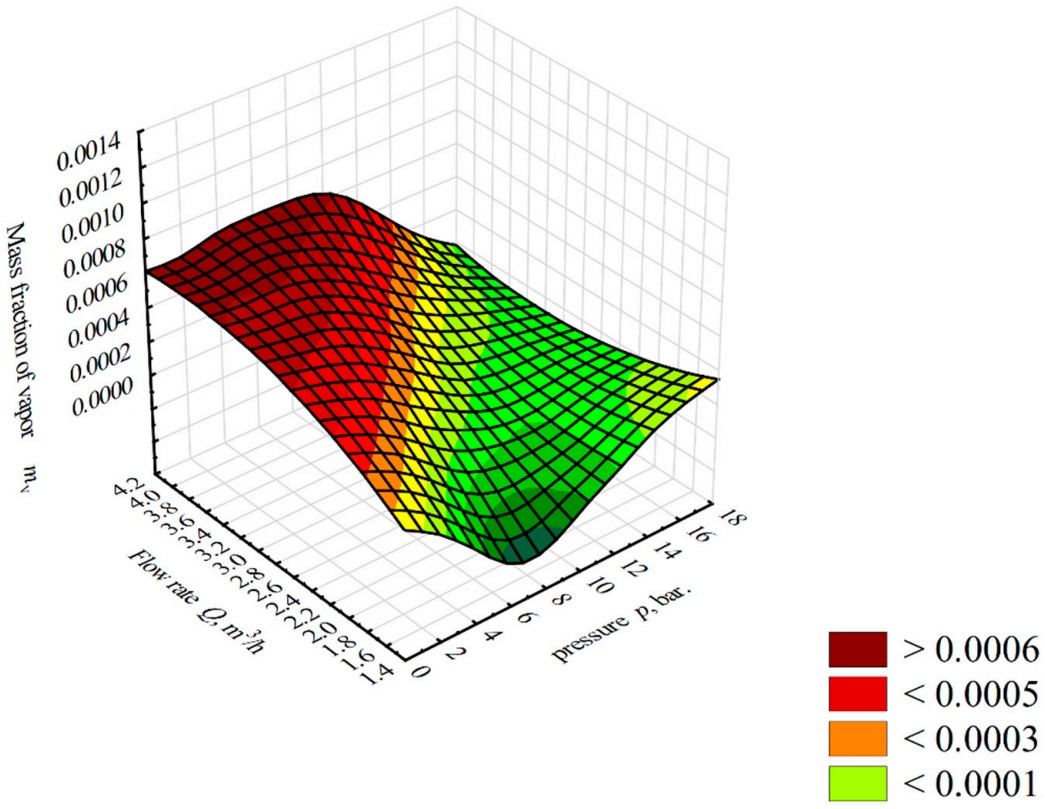

Figure 7. 3D contour plot of the mass fraction of vapor m_v against the flow rate Q and the pressure p.

3.2. Desulfurisation of a Pyrolysis Oil

After inserting the optimized Venturi tube into the cavitator of the plant (see Figure 2), three different cavitation conditions with different oil-water mixing ratios were tested.

For the developed process, the effects of parameters such as pressure drop, process duration, and oil volume fraction are believed to be most crucial, and the results pertaining to these are given in Figures 8–10. There was a tendency for desulfurization efficiency to increase with increasing inlet pressure (Figures 8–10). When the tire pyrolysis oils were 2.5% in the oil-water mixture and the inlet pressure of 3 bar, the desulfurization efficiency was at 5.43%. Increasing the inlet pressure to 4 bar increased the efficiency to 6.75%, and increasing it to 5 bar further increased the efficiency to 7.46%. The same trend was obtained when the oils were 5.0 and 7.5% in the oil-water mixture. Maximum desulfurization efficiency was determined at 5 bars inlet pressure when the oil was 5.0% in the maximum efficiency was 9.87% and at 7.5% of oil, respectively 32.29%. The overall efficiency is empowered by the amount of vapor, including water and tire pyrolysis oil, that diffuses into the cavity, increases with the larger expansion of the bubbles where the cavitation zone is developed. This provides an enlarged active volume for oxidation reaction [51]. This leads to the intensification of the radical formation reactions and to the formation of a fine emulsion, which facilitates the oxidation phase [46].

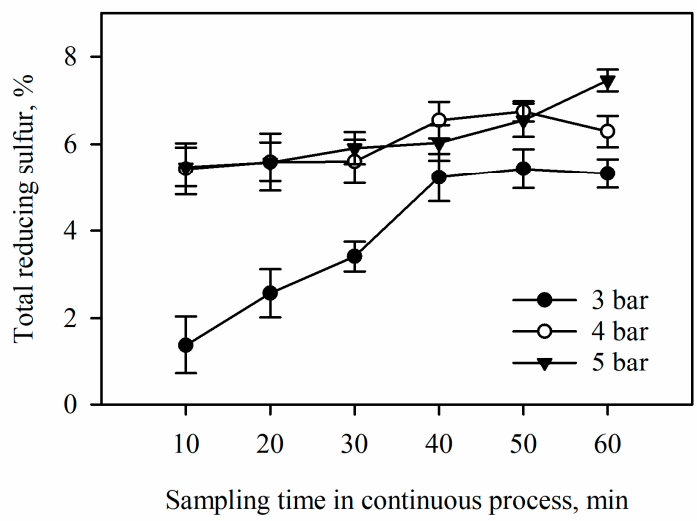

Figure 8. Effect of desulfurization at 2.5% tire pyrolysis oil volume.

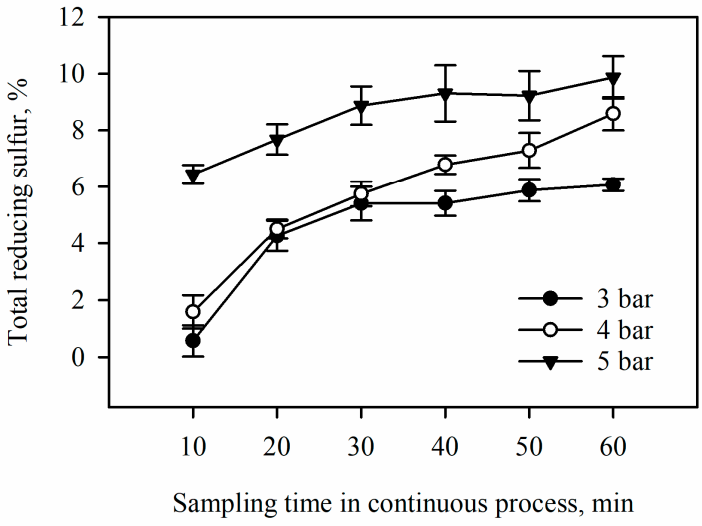

Figure 9. Effect of desulfurization at 5.0% tire pyrolysis oil volume.

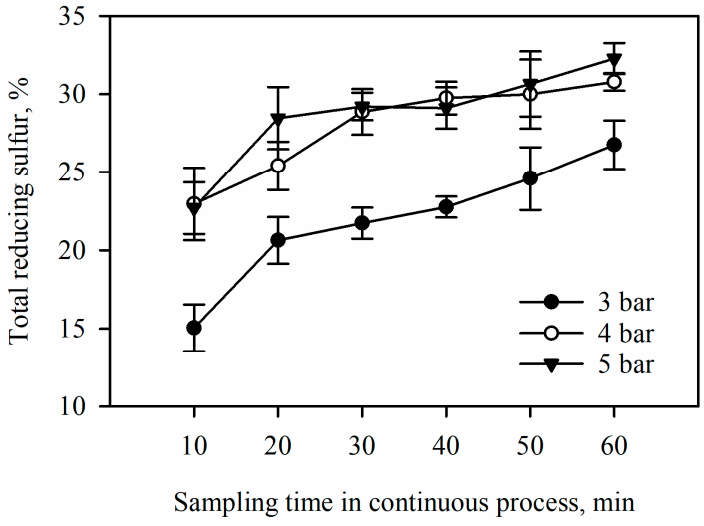

Figure 10. Effect of desulfurization at 7.5% tire pyrolysis oil volume.

At a higher inlet pressure of 6 bar, no further increase could be achieved. It is probably present as described by [46]. Following the increase in pressure, the cavitation zone is excessively filled with a large number of cavities. Herein, the cavities containing kerosene and/or water vapor molecules coalescence to form a cavity cloud. This large cavity cloud escapes the reactor without enduring collapses. As a result, decay in overall intensity occurs via the incomplete or cushioned collapse of the cavities.

The process duration of the treatment is another major challenge of oxidative desulfurization that directly affects the efficiency and the most economic aspects of the process. The effect of the treatment time within the interval of 10–60 min at various hydrodynamic cavitation inlet pressures (3–5 bar) can also be determined by comparing Figures 8–10. In all experiments, a tendency to increase the desulfurization efficiency with increasing treatment time was observed. This is attributed to the improved interaction of the two immiscible phases of tire pyrolysis oil and water (more hydroxyl radicals are formed). This results in the progression of the oxidation reaction and facilitates the transfer of polar oxidized sulfur compounds to the aqueous phase [46]. However, this trend slows down for further treatment time (from 30 min). Assessing the duration of the process, the data we obtained have the same trend as [46] but contradict the report of [52], who observed a decay in sulfur removal with an increase in duration time beyond a certain limit.

3.3. Interactive Effects Analysis

The results obtained from the analysis of desulfurization as a function of the individual parameters of exposure time, inlet pressure, and oil/water ratio do not seem to be describable by simple analytical relations. Rather, interactive effects or dependencies of the parameters seem to exist. Therefore 3D dimensional response plots were developed. Surface plots were used, with only the two parameters in Figure 11a–c shown in 2D. The extent of desulfurization was color-coded, and the numerical extent was given in percent.

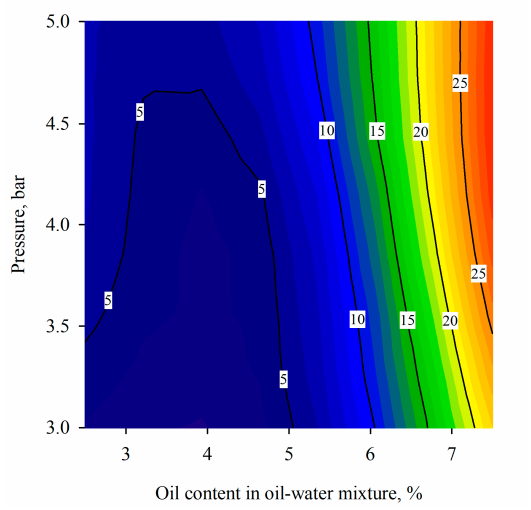

Figure 11. (**a**–**c**) Response surface 2D graph; the interactive effect of pressure, oil content in oil-water mixture, and duration time on desulfurization.

The interaction effect of the pressure and oil content in the oil-water mixture can be estimated from Figure 11a. The beneficial effect of increasing both parameters in parallel is achieved to the maximum value. The observed trend can be related to the increased oxidation intensity due to the physical action of hydrodynamic cavitation by stirring the chip and the formation of a large intercellular area between the tire pyrolysis oil and the water mixture. The results show that the effect of inlet pressure was found to be rather negligible at low values of oil to aqueous phase volume ratio (2.5 and 5.0%). More than 30% of the sulfur is removed at the same time as setting the inlet pressure above 4.5 bar with 7.5% oil in a mixture of oil and water. Thus, based on observations and modeling results, in order to maximize sulfur oxidation, not only the oil content of the oil-water mixture but also the contribution of inlet pressure needs to be considered.

Figure 11b depicts the mutual effect of inlet pressure and duration time with the effect of desulfuring. Accordingly, the extent of sulfur oxidation is less sensitive to changes in pressure at a shorter duration time. Only with increasing reaction times does the sensitivity to changes in the input pressure increase. This means that the reaction time can be shortened by increasing the inlet pressure to remove the sulfur content. Achieving >30% sulfur removal is possible in oxidation time 55 min, setting the inlet pressure within the range of 4.4–5 bar. However, this conclusion was also found in the single parameter analysis in Section 3.2, so that there is probably no strong interaction between the input pressure and duration time parameters with regard to their effect on desulfurization.

The interaction of tire pyrolysis oil in oil-water mixture and duration time is described in Figure 11c. The diagram shows that the effect of process time is almost imperceptible up to an oil content of 5.5% in the oil-water mixture. Only at higher oil contents does the extent of desulfurization increase significantly. The maximum effect of sulfur removal occurs at an oil content of 7.0%, which contrasts with [38], who found a maximum effect with only 2.5% organic content. However, [38] was able to achieve quantitative desulfurization with that low organic content after 60 min [38]. Other studies, such as [53], explain that the mechanism of desulfurization by hydrodynamic cavitation is very complex due to the many technical parameters and their influence on the chemical-physical properties of the water-oil mixture, which differs from the mechanisms of the sister technology of acoustic cavitation. As [38,53] conclude, an additional cosolvent or other additives could increase the desulfurization yield, which is the subject of further investigations by the authors.

4. Conclusions

In this study, a cavitation system was constructed, and the core of the system, the Venturi tube, was modified based on simulation calculations and printed from PLA. The results of the numerical simulation showed that the cavitation phenomenon is excited in the pressure range of 3–6 bar and in the flow range 2.5–4 $m^3\ h^{-1}$, whereby the flow rate has a greater influence on cavitation than the inlet pressure. However, the simulation only took into account the vapor pressure of the water as the only medium. Furthermore, instead of "simple", chemically homogeneous alkane mixtures such as diesel fuel or paraffin, a pyrolysis oil from used tires was used, which is typically characterized by a high reactivity and an associated low storage stability. As was found during these investigations into the desulfurization of pyrolysis oil from used tires, the maximum working pressure of the cavitation system is limited by the pyrolysis oil to less than 6 bar. After a 60-min treatment at a pressure of 5 bar before the cavitation tool, almost 33% of the oil could be desulfurized with the help of the cavitation system. Shorter treatment times and an inlet pressure of less than 4 bar resulted in smaller desulfurization yields. Furthermore, the interaction analysis showed that only from a pyrolysis oil content of 5.5 to 6% the hydrodynamic cavitation has an effective effect on the desulfurization.

Author Contributions: Conceptualization, A.Ž., A.S.; methodology, E.B., R.R., V.J.; Data curation, J.U., Ž.K., J.J., E.B., R.R. and A.S.; validation, J.U., Ž.K., J.J., A.Ž. and R.R.; formal analysis, J.U., Ž.K., J.J., A.Ž., E.B. and R.R.; investigation, J.U., Ž.K., J.J., A.Ž., E.B. and R.R.; writing—original draft preparation, J.U., Ž.K., J.J. and A.Ž.; visualization, J.U., Ž.K., J.J. and E.B.; supervision, J.U., Ž.K., J.J.

and A.Ž.; resources, V.J. A.S.; funding acquisition, J.U., Ž.K., J.J. and A.Ž. All authors have read and agreed to the published version of the manuscript.

Funding: This research received no external funding.

Institutional Review Board Statement: Not applicable.

Informed Consent Statement: Not applicable.

Data Availability Statement: Not applicable.

Conflicts of Interest: The authors declare no conflict of interest.

References

1. Svanberg, M.; Ellis, J.; Lundgren, J.; Landval, I. Renewable methanol as a fuel for the shipping industry. *Renew. Sustain. Energy Rev.* **2018**, *94*, 1217–1228. [CrossRef]
2. Sahin, B.; Yilmaz, H.; Ust, Y.; Fuat Guneri, A.; Gulsun, B.; Turan, E. An Approach for Economic Analysis of Intermodal Transportation. *Sci. World J.* **2014**, *2014*, 630320. [CrossRef]
3. IMO. UN Body Adopts Climate Change Strategy for Shipping IMO. 13 April 2018. Available online: https://www.imo.org/en/MediaCentre/PressBriefings/Pages/06GHGinitialstrategy.aspx (accessed on 30 June 2021).
4. *Decarbonising Maritime Transport Pathways to Zero-Carbon Shipping by 2035 Pathways to Zero-Carbon Shipping by 2035*; International Transport Forum: Paris, France, 2018; Available online: https://www.itf-oecd.org/sites/default/files/docs/decarbonising-maritime-transport-2035.pdf (accessed on 30 June 2021).
5. Mallouppas, G.; Yfantis, E.A. Decarbonization in Shipping Industry: A Review of Research, Technology Development, and Innovation Proposals. *J. Mar. Sci. Eng.* **2021**, *9*, 415. [CrossRef]
6. Gilbert, P.; Walsh, C.; Traut, M.; Kesieme, U.; Pazouki, K.; Murphy, A. Assessment of full life-cycle air emissions of alternative shipping fuels. *J. Clean. Prod.* **2018**, *172*, 855–866. [CrossRef]
7. Yaqoob, H.; Teoh, Y.H.; Sher, F.; Jamil, M.A.; Murtaza, D.; Al Qubeissi, M.; UI Hassan, M.; Mujtaba, M.A. Current Status and Potential of Tire Pyrolysis Oil Production as an Alternative Fuel in Developing Countries. *Sustainability* **2021**, *13*, 3214. [CrossRef]
8. European Commission. *Council Directive 1999/31/EC on the Landfill of Waste*; European Commission: Brussels, Belgium, 1999; Available online: https://eur-lex.europa.eu/legal-content/EN/TXT/?uri=CELEX:01999L0031-20180704 (accessed on 26 June 2021).
9. Bulei, C.; Todor, M.P.; Heput, T.; Kiss, I. Directions for material recovery of used tires and their use in the production of new products intended for the industry of civil construction and pavements. *IOP Conf. Ser. Mater. Sci. Eng.* **2018**, *294*, 012064. [CrossRef]
10. Fazli, A.; Rodrigue, D. Recycling Waste Tires into Ground Tire Rubber (GTR)/Rubber Compounds: A Review. *J. Compos. Sci.* **2020**, *4*, 103. [CrossRef]
11. Martinez, J.D.; Puy, N.; Murillo, R.; Garcia, T.; Navarro, M.V.; Mastral, A.M. Waste tyre pyrolysis—A review. *Renew. Sustain. Energy Rev.* **2013**, *23*, 179–213. [CrossRef]
12. Ramos, G.; Alguacil, E.J.; Lopez, F.A. The recycling of end-of-life tyres. technological review. *Rev. Metal.* **2011**, *47*, 273. [CrossRef]
13. Ranzi, E.; Dente, M.; Faravelli, T.; Bozzano, G.; Fabini, S.; Nava, R.; Cozzani, V.; Tognotti, L. Kinetic modelling of polyethylene and polypropylene thermal degradation. *J. Anal. Appl. Pyrolysis* **1997**, *40*, 305–319. [CrossRef]
14. Jouhara, H.; Ahmad, D.; van den Boogaert, I.; Katsou, E.; Simons, S.; Spencer, N. Pyrolysis of domestic based feedstock at temperatures up to 300 °C. *Therm. Sci. Eng. Prog.* **2018**, *5*, 117–143. [CrossRef]
15. Kloss, S.; Zehetner, F.; Dellantonio, A.; Hamid, R.; Ottner, F.; Liedtke, V.; Schwanninger, M.; Gerzabek, M.H.; Soja, G. Characterization of Slow Pyrolysis Biochars: Effects of Feedstocks and Pyrolysis Temperature on Biochar Properties. *J. Environ. Qual.* **2012**, *41*, 990–1000. [CrossRef]
16. Suriapparao, D.V.; Vinu, R. Effects of Biomass Particle Size on Slow Pyrolysis Kinetics and Fast Pyrolysis Product Distribution. *Waste Biomass Valorization* **2018**, *9*, 465–477. [CrossRef]
17. Li, X.W.C.; Li, Z.; Yu, G.; Wang, Y. Effect of pyrolysis temperature on characteristics, chemical speciation and risk evaluation of heavy metals in biochar derived from textile dyeing sludge. *Ecotoxicol. Environ. Saf.* **2019**, *168*, 45–52. [CrossRef]
18. Meier, D.; Faix, O. State of the art of applied fast pyrolysis of lignocellulosic materials—A review. *Bioresour. Technol.* **1999**, *68*, 71–77. [CrossRef]
19. Qureshi, K.M.; Ng Kay Lup, A.; Khan, S.; Abnisa, F.; Daud, W.M.A.W. A technical review on semi-continuous and continuous pyrolysis process of biomass to bio-oil. *J. Anal. Appl. Pyrolysis* **2018**, *131*, 52–75. [CrossRef]
20. Das, P.; Tiwari, P. The effect of slow pyrolysis on the conversion of packaging waste plastics (PE and PP) into fuel. *Waste Manag.* **2018**, *79*, 615–624. [CrossRef]
21. Barry, D.; Barbiero, C.; Briens, C.; Berruti, F. Pyrolysis as an economical and ecological treatment option for municipal sewage sludge. *Biomass Bioenergy* **2019**, *122*, 472–480. [CrossRef]
22. Chua, H.S.; Bashir, M.J.K.; Tan, K.T.; Chua, H.S. A sustainable pyrolysis technology for the treatment of municipal solid waste in Malaysia. *AIP Conf. Proc.* **2019**, *2124*, 020016. [CrossRef]

23. Samolada, M.C.; Zabaniotou, A.A. Comparative assessment of municipal sewage sludge incineration, gasification and pyrolysis for a sustainable sludge-to-energy management in Greece. *Waste Manag.* **2014**, *34*, 411. [CrossRef]
24. Jeswani, H.; Krüger, C.; Russ, M.; Horlacher, M.; Antony, F.; Hann, S.; Azapagic, A. Life cycle environmental impacts of chemical recycling via pyrolysis of mixed plastic waste in comparison with mechanical recycling and energy recovery. *Sci. Total Environ.* **2021**, *769*, 144483. [CrossRef]
25. Jantaraksa, N.; Prasassarakich, P.; Reubroycharoen, P.; Hinchiranan, N. Cleaner alternative liquid fuels derived from the hydrodesulfurization of waste tire pyrolysis oil. *Energy Convers. Manag.* **2015**, *95*, 424–434. [CrossRef]
26. Directive 2008/98/EC of the European Parliament and of the Council of 19 November 2008 on Waste and Repealing Certain Directives. Available online: https://eur-lex.europa.eu/eli/dir/2008/98/oj (accessed on 24 June 2021).
27. Dobrotă, D.; Dobrotă, G. An innovative method in the regeneration of waste rubber and the sustainable development. *J. Clean. Prod.* **2018**, *172*, 3591–3599. [CrossRef]
28. Frigo, S.; Seggiani, M.; Puccini, M.; Vitolo, S. Liquid fuel production from waste tyre pyrolysis and its utilisation in a Diesel engine. *Fuel* **2014**, *116*, 399–408. [CrossRef]
29. Kumaravel, S.T.; Murugesan, A.; Kumaravel, A. Tyre pyrolysis oil as an alternative fuel for diesel engines—A review. *Renew. Sustain. Energy Rev.* **2016**, *60*, 1678–1685. [CrossRef]
30. Quek, A.; Balasubramanian, R. Liquefaction of waste tires by pyrolysis for oil and chemicals—A review. *J. Anal. Appl. Pyrolysis* **2013**, *101*, 1–16. [CrossRef]
31. Antoniou, N.; Zabaniotou, A. Features of an efficient and environmentally attractive used tyres pyrolysis with energy and material recovery. *Renew. Sustain. Energy Rev.* **2013**, *20*, 539–558. [CrossRef]
32. Official Journal L 076, 22/03/2003, Directive 2003/17/EC of the European Parliament and of the Council of 3 March 2003 Amending Directive 98/70/EC Relating to the Quality of Petrol and Diesel Fuels. Available online: https://eur-lex.europa.eu/eli/dir/2003/17/oj (accessed on 24 June 2021).
33. Diaz de Leon, J.N.; Kumar, C.R.; Antunez-Garcia, J.; Fuentes-Moyado, S. Recent Insights in Transition Metal Sulfide Hydrodesulfurization Catalysts for the Production of Ultra Low Sulfur Diesel: A Short Review. *Catalysts* **2019**, *9*, 87. [CrossRef]
34. Hossain, M.N.; Park, H.C.; Choi, H.S. A Comprehensive Review on Catalytic Oxidative Desulfurization of Liquid Fuel Oil. *Catalysts* **2019**, *9*, 229. [CrossRef]
35. Kumar, S.; Chandra Srivastava, V.; Madhusudan Nanoti, S. Extractive Desulfurization of Gas Oils: A Perspective Review for Use in Petroleum Refineries. *Sep. Purif. Rev.* **2017**, *46*, 319–347. [CrossRef]
36. Aitani, A.M.; Ali, M.F.; Al-Ali, H.H. A review of non conventional methods for the desulfurization of residual fuel oil. *Petrol. Sci. Technol.* **2000**, *18*, 537–553. [CrossRef]
37. Chandra Srivastava, V. An evaluation of desulphurization technologies for sulphur removal from liquid fuels. *RSC Adv.* **2012**, *2*, 759–783. [CrossRef]
38. Suryawanshi, N.; Bhandari, V.; Sorokhaibam, L.; Ranade, V.V. A Non-catalytic Deep Desulphurization Process using Hydrodynamic Cavitation. *Sci. Rep.* **2016**, *6*, 33021. [CrossRef] [PubMed]
39. Sun, X.; Park, J.J.; Kim, H.S.; Lee, S.H.; Seong, S.J.; Om, A.S.; Yoon, J.Y. Experimental investigation of the thermal and disinfection performances of a novel hydrodynamic cavitation reactor. *Ultrason. Sonochem.* **2018**, *49*, 13–23. [CrossRef]
40. Talebian Gevari, M.; Abbasiasl, T.; Niazi, S.; Ghorbani, M.; Kosar, A. Direct and indirect thermal applications of hydrodynamic and acoustic cavitation: A review. *Appl. Therm. Eng.* **2020**, *171*, 115065. [CrossRef]
41. Albanese, L.; Ciriminna, R.; Meneguzzo, F.; Pagliaro, M. Beer-brewing powered by controlled hydrodynamic cavitation: Theory and real-scale experiments. *J. Clean. Prod.* **2016**, *142*, 1457–1470. [CrossRef]
42. Albanese, L.; Ciriminna, R.; Meneguzzo, F.; Pagliaro, M. Energy efficient inactivation of Saccharomyces cerevisiae via controlled hydrodynamic cavitation. *Energy Sci. Eng.* **2015**, *3*, 221–238. [CrossRef]
43. Carpenter, J.; Badve, M.; Rajoriya, S.; George, S.; Kumar Saharan, V.; Pandit, A.B. Hydrodynamic cavitation: An emerging technology for the intensification of various chemical and physical processes in a chemical process industry. *Rev. Chem. Eng.* **2016**, *33*, 433–468. [CrossRef]
44. Pokhrel, N.; Vabbina, P.K.; Pala, N. Sonochemistry: Science and Engineering. *Ultrason. Sonochem.* **2016**, *29*, 104–128. [CrossRef]
45. Suslick, K.S.; Mdleleni, M.M.; Ries, J.T. Chemistry induced by hydrodynamic cavitation. *J. Am. Chem. Soc.* **1997**, *119*, 9303–9304. [CrossRef]
46. Baradaran, S.; Sadeghi, M.T. Desulfurization of non-hydrotreated kerosene using hydrodynamic cavitation assisted oxidative desulfurization (HCAOD) process. *J. Environ. Chem. Eng.* **2020**, *8*, 103832. [CrossRef]
47. Kozyuk, O.V. Desulphurization Process and Systems Utilizing Hydrodynamic Cavitation. U.S. Patent 8,002,971 B2, 23 August 2011.
48. Kulkarni, A.A.; Ranade, V.V.; Rajeev, R.; Koganti, S.B. CFD Simulation of Flow in Vortex Diodes. *AIChE J.* **2008**, *54*, 1139–1152. [CrossRef]
49. Wang, J.; Chen, W. Numerical optimization design of vortex diode hydrodynamic cavitation reactor. *J. Phys. Conf. Ser.* **2019**, *1300*, 012116. [CrossRef]
50. Sun, X.; Hyeok Kang, C.; Jin Park, J.; Soo Kim, H.; Son Om, A.; Yong Yoon, J. An experimental study on the thermal performance of a novel hydrodynamiccavitation reactor. *Exper. Therm. Fluid Sci.* **2018**, *99*, 200–210. [CrossRef]

51. Soyama, H.; Hoshino, J. Enhancing the aggressive intensity of hydrodynamic cavitation through a Venturi tube by increasing the pressure in the region where the bubbles collapse. *AIP Adv.* **2016**, *6*, 045113. [CrossRef]
52. Ja'fari, M.; Ebrahimi, S.L.; Khosravi-Nikou, M.R. Ultrasound-assisted oxidative desulfurization and denitrogenation of liquid hydrocarbon fuels: A critical review. *Ultrason. Sonochem.* **2018**, *40*, 955–968. [CrossRef]
53. Abramov, V.O.; Abramov, A.V.; Cravotto, G.; Nikonov, R.V.; Fedulov, I.S.; Ivanov, V.K. Flow-mode water treatment under simultaneous hydrodynamic cavitation and plasma. *Ultrason. Sonochem.* **2021**, *70*, 105323. [CrossRef]